

Strategy persistence-consistency and reputation promote cooperation in dual-layer networks for prisoner's dilemma games

Qianwei Zhang(张倩伟), Jiaqi Liu(刘佳琪), and Leiman Fu(付蕾蔓)
Citation: Chin. Phys. B, 2025, 34 (**12**): 120201. DOI: 10.1088/1674-1056/ade665
http://cpb.iphy.ac.cn; http://iopscience.iop.org/cpb

What follows is a list of articles you may be interested in

Impact of peer pressure on cooperation evolution in the networked prisoner's dilemma game with migration mechanisms

Xianjia Wang(王先甲), Yanan Li(李亚楠), and Zhipeng Yang(杨志鹏)
Chin. Phys. B, 2025, 34 (**11**): 110201. DOI: 10.1088/1674-1056/ade425

Generic stability of cooperative equilibria for multi-leader-follower-population mixed games

Wenjun Wu(武文俊), Hui Yang(杨辉), and Guanghui Yang(杨光惠)
Chin. Phys. B, 2025, 34 (**10**): 100202. DOI: 10.1088/1674-1056/ade666

Influence of conformity on the evolution of cooperation in games with sampling rules on networks

Xianjia Wang(王先甲) and Qiaoyu He(何翘愚)
Chin. Phys. B, 2025, 34 (**3**): 030202. DOI: 10.1088/1674-1056/ada42e

Non-monotonic behavior of jam probability and stretched exponential distribution in pedestrian counterflow

Ze-Hao Chen(陈泽昊), Zhi-Xi Wu(吴枝喜), and Jian-Yue Guan(关剑月)
Chin. Phys. B, 2024, 33 (**9**): 090206. DOI: 10.1088/1674-1056/ad57ab

Evolutionary dynamics of tax-based strong altruistic reward and punishment in a public goods game

Zhi-Hao Yang(杨智昊) and Yan-Long Yang(杨彦龙)
Chin. Phys. B, 2024, 33 (**9**): 090205. DOI: 10.1088/1674-1056/ad5274

Strategy persistence-consistency and reputation promote cooperation in dual-layer networks for prisoner's dilemma games

Qianwei Zhang(张倩伟), Jiaqi Liu(刘佳琪), and Leiman Fu(付蕾蔓)†

School of Mathematics, Renmin University of China, Beijing 100872, *China*

(Received 16 March 2025; revised manuscript received 10 May 2025; accepted manuscript online 20 June 2025)

We propose a dual-layer network model that integrates social and familial contexts, consisting of a social interaction layer and a family relationship layer. We design a reputation-based incentive mechanism incorporating strategy persistence-consistency to investigate how reputation fosters cooperation. The model features the following aspects: (1) a dynamic disconnection–reconnection mechanism in the social layer, (2) a reputation-enhanced Fermi rule in the family layer, and (3) a refined partitioning of the family network. Simulation results indicate that the disconnection–reconnection parameter (σ) significantly enhances cooperation in the social network; the strategic persistence-consistency influencing factor (α) has a positive impact on cooperation in both layers; and moderately dividing the family network promotes the emergence of cooperation. The research findings facilitate group cooperation in complex networks and offer valuable insights for addressing social dilemmas in the real world.

Keywords: prisoner's dilemma, dual-layer network, disconnection–reconnection mechanism, strategy persistence-consistency

PACS: 02.50.Le

DOI: 10.1088/1674-1056/ade665 **CSTR:** 32038.14.CPB.ade665

1. Introduction

Darwin's theory posits that natural selection favors individuals who maximize their self-interest by adopting a defection strategy.[1] Paradoxically, cooperation prevails across both biological and social systems, challenging classical evolutionary frameworks. Evolutionary game theory (EGT) resolves this contradiction by elucidating how cooperation emerges from conflicts between individual and collective interests. Canonical models — the prisoner's dilemma,[2–6] the public goods game,[7–9] stag hunting,[10] and the snowdrift game[11–13] — quantify cooperative mechanisms, extending the explanatory power of EGT from natural ecosystems to human societal behaviors.

Researchers have proposed various mechanisms, including memory effects,[14–16] reward–punishment systems,[17–20] conformity,[21–23] emotion[24–26] and reputation,[27–33] in order to explain the evolution of cooperative behavior. Reputation is ubiquitous in society, and individuals' decisions directly shape their perceived credibility. Recent studies emphasize the role of strategic persistence in reputation formation. For instance, Bi and Yang[28] proposed a heterogeneity-driven mechanism linking strategic persistence to reputation, demonstrating enhanced cooperation through persistent behavioral patterns. He *et al.*[31] developed a reputation-based strategy persistence model in which current reputation increments depend on historical adherence to strategies. Zhang *et al.*[32] integrated strategic persistence into spatial prisoner's dilemma scenarios, revealing that individuals with extreme reputations (either high or low) exhibit heightened strategic volatility.

Complex network theory has significantly advanced EGT research. Traditional network models typically feature static, single-layer topologies where nodes interact within isolated infrastructures — a simplification that is often insufficient for capturing the intricacies of real-world systems.[34] In contrast, multilayer networks account for the complexity of interconnected systems through intra-layer and inter-layer connections. Current research on multilayer networks encompasses interconnected networks,[35–38] interdependent networks[39–48] and multiplex networks.[49] For example, Wang *et al.*[45] studied the evolution of cooperation in public goods games on interdependent networks and found that introducing a reputation reasoning mechanism enhances cooperation levels. Chowdhury *et al.*[46] simulated individuals' behaviors across different network layers under various evolutionary games, considering individuals' movements within network layers to improve their fitness. Ge *et al.*[47] examined irregular cumulative strategies in interdependent networks, demonstrating that strategic differences across layers significantly enhance cooperation.

As a core mechanism in EGT, the disconnection–reconnection mechanism allows individuals to dynamically adjust network connections based on factors such as reputation and strategic payoffs.[50–56] Zimmermann *et al.*[50] introduced the concept of network plasticity, where existing connections can be altered or replaced based on the total pay-

†Corresponding author. E-mail: fuleiman@ruc.edu.cn

© 2025 Chinese Physical Society and IOP Publishing Ltd. All rights, including for text and data mining, AI training, and similar technologies, are reserved.

offs of interacting elements. Studies indicate that incorporating local neighbor selection in network adaptation dynamics fosters small-world attributes, leading to a more stable state with increased cooperation. Pan *et al.*[52] investigated the impact of spatially adaptive interactions on cooperation in the prisoner's dilemma. The findings reveal that increasing the likelihood of players refusing to engage with neighbors can effectively bolster cooperators' resistance to defection, thereby stabilizing cooperation. Zhang *et al.*[56] examined small-world networks, showing that increasing probability of rewiring significantly enhances the effectiveness of reputation-driven disconnection–reconnection mechanisms.

Individuals play different roles in societies and families, leading to diverse interpersonal interactions. For example, some may excel at work but display poor behavior at home, while others may be driven by profit in society yet can maintain a harmonious family life. Evaluating such individuals requires considering their reputation across different contexts. Social relationships are fluid, allowing disconnection and reconnection, whereas family ties are more stable. Considering these differences, we propose a dual-layer network model that consists of a social interaction layer and a family relationship layer, where individuals face different neighbors in each network. In the social layer, the disconnection–reconnection mechanism ensures that the probability of two players establishing a connection depends on reputation gaps relative to the environment. In the family layer, strategies are updated via a Fermi rule incorporating reputation differences. Players' reputations are updated holistically based on their performance across both layers.

The rest of the paper is structured as follows. In Section 2, we describe the model in detail. Then in Section 3, we analyze the simulation results. Finally in Section 4, we summarize the research findings.

2. Model

We consider a spatial prisoner's dilemma model on a dual-layer square-lattice network. Each layer of the square-lattice network consists of the same $N = L^2$ uniformly distributed players, but players are located in different positions in each layer. As shown by the red dots in Fig. 1(a), the neighborhood relationships differ between the social layer (upper layer) and family layer (lower layer). In both layers, blue dots represent a player's neighbors in the social layer while hollow dots denote other network participants.

To reflect real-world social dynamics where interpersonal connections are transient, the social layer employs dashed lines to indicate unstable links that may disconnect and reconnect randomly. In contrast, family relationships exhibit greater stability — shown by solid lines in the lower layer — as people rarely sever or extend kinship ties abruptly. Color-coded grids (e.g., yellow and purple in Fig. 1(a)) represent distinct family units, with edge gaps between differently colored regions indicating no inter-family connections. Figure 1(b) details the network structure of the family layer. The square lattice is partitioned into non-overlapping 2×2 sub-lattices, each representing a family unit. Dashed division lines separate different families. The social layer network and all sub-networks in the family layer adopt periodic boundary conditions.

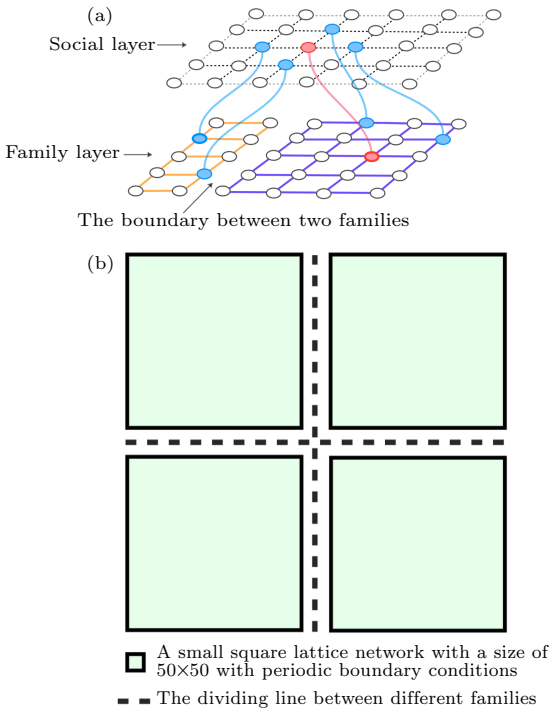


Fig. 1. Schematic diagram of the dual-layer network structure. (a) Schematic diagram of social layer and family layer networks. (b) Schematic diagram of family layer network partition.

Initially, players choose to cooperate (C) or defect (D) with equal probability in both layers. Without loss of generality, we adopt the weak prisoner's dilemma payoff matrix

$$M = \begin{pmatrix} 1 & 0 \\ b & 0 \end{pmatrix}, \tag{1}$$

where $b > 1$. The payoff of player x at each time step is defined as

$$\pi_x^i = \sum_{y \in N_x} \pi_{xy}^i. \tag{2}$$

Here, N_x denotes player x's neighbor set, π_{xy} is the payoff form interactions with neighbor y, $i \in \{1,2\}$ indicates the network layer ($i = 1$ refers to the social layer and $i = 2$ refers to the family layer).

In the social layer, players dynamically adjust connections based on their own reputation and neighbors' reputations. If both players' reputations fall below the environmental reputation, indicating a collectively poor reputation, their disconnection probability increases. Conversely, if both reputations surpass the environmental reputation, indicating a collectively positive reputation, connection probability rises. According to

the definition in Ref. [56], the environmental reputation $\overline{R_{xy}}(t)$ of players x and y in the social layer at time t is defined as follows:

$$\overline{R_{xy}}(t)=\frac{\sum\limits_{z\in N_x^1\cup N_y^1}R_z(t)}{\left|N_x^1\cup N_y^1\right|}, \tag{3}$$

where $N_x^1\cup N_y^1$ includes all neighbors and the players themselves in the social layer and $\left|N_x^1\cup N_y^1\right|$ denotes the number of elements in this set.

The probability of successful connection between players x and y is calculated using the following formula:

$$P_{xy}(t)=\frac{1}{2}\left[1+\mathrm{erf}\frac{\left(R_x(t)+R_y(t)\right)/2-\overline{R_{xy}}(t)}{\sigma\sqrt{2}}\right], \tag{4}$$

where $\mathrm{erf}(x)=\frac{2}{\sqrt{\pi}}\int_0^x \mathrm{e}^{-t^2}\mathrm{d}t$. The parameter σ (selection intensity) corresponds to the standard deviation of the normal distribution, characterizing how the average reputation of players x and y interacts with environmental reputation to determine their connection probability. When the average reputation $\overline{R_{xy}}(t)$ equals the environmental reputation, the system exhibits a neutral connectivity state with a connection probability of exactly 50%. Positive deviations ($\overline{R_{xy}}(t)>R_{\mathrm{env}}$) increase the probability above 0.5, while negative deviations reduce it below this threshold. The parameter σ modulates the system's sensitivity: larger σ values yield gradual probability transitions across reputation differences, resulting in a smooth response curve; smaller σ values cause abrupt probability shifts, creating steep transitions between high and low connectivity states under equivalent reputation disparities. When $\sigma\to 0$, if the average reputation value of player x and y is lower than the environmental reputation, the connection probability $P_{xy}(t)\to 0$; if the average reputation value is higher, $P_{xy}(t)\to 1$. This shows that individual and environmental reputation significantly regulate connections. However, when $\sigma\to\infty$, $P_{xy}(t)\to 0.5$, connections become random, and the disconnection–reconnection mechanism loses its effect.

Next, the update rules for network reputations in both layers are introduced. First, consider strategy persistence and consistency. Since the strategies chosen by players in the past influence their current reputation, strategies chosen in one layer also influence the reputation in another layer. We introduce the strategy persistence-consistency parameter d,

$$d_x(t)=\begin{cases} d_x(t-1)+0.1, & \text{if } s_x^1(t-1)=s_x^1(t)=s_x^2(t-1)=s_x^2(t),\\ 1, & \text{otherwise,}\end{cases} \tag{5}$$

where $s_x^1(t)$ is the decision made by player x in the social layer at time t and $s_x^2(t)$ is the decision made by player x in the family layer at time t. Formula (5) shows that only when the player's strategies in both layers are consistent across two consecutive time steps does the persistence-consistency parameter d increases by 0.1. Through simulations, when the upper limit of the consistency parameter d is small, defectors easily dominate, leading to full defection. When the upper limit of d is too large, cooperators quickly dominate, causing full cooperation (the reputation of consistent two-layer network cooperators is overly high), which is unrealistic. Given this, we set the upper limit of d to 3.[57] That is, when $d_x(t)\geq 3$, we set $d_x(t)=3$.

In the process of reputation updating, each layer's reputation is affected by the player's strategy choices in both layers, i.e., social reputation and family reputation affect each other. In reality, the fluctuation of reputation is not fixed. Judgments of a person often refer to their historical actions in multiple environments. To be specific, if one consistently adopts the same strategy in society and family, and is regarded as a "thoroughgoing" good or bad person, his persistence-consistency parameter d will grow within a certain range. Conversely, if one presents different images in society and family or acts inconsistently in two choices, his behavior will be doubted and only their current action will be evaluated. Based on this analysis, reputation updates follow: if C is chosen in both layers, reputations in both layers increase; if D is chosen in both, reputations in both layers decrease; if the player's strategy choices in the two layers are different, it indicates that the player's behavior is inconsistent, then the reputation will increase in the cooperation layer and decrease in the betrayal layer. The specific representation is as follows:

$$R_x^i(t)=\begin{cases} R_x^i(t-1)+\alpha d_x(t), & \text{if } s_x^i(t)=C,\\ R_x^i(t-1)-\alpha d_x(t), & \text{if } s_x^i(t)=D,\end{cases} \tag{6}$$

where α is the strategy persistence-consistency influencing factor, $R_x^i(t)$ represents the reputation of player x in each layer, $i=1$ is the social layer, and $i=2$ is the family layer. To ensure that individual reputation does not increase or decrease indefinitely, a reputation cap H is introduced. When $R_x(t)\geq H$, we set $R_x(t)=H$; and when $R_x(t)\leq 0$, we set $R_x(t)=0$. In this study, we set $H=40$.[56]

Strategy updates follow a Fermi function where players imitate neighbors probabilistically. The probability that player x learns the strategy of neighbor y is

(i) in social layer:

$$W(s_y\to s_x)=\frac{1}{1+\exp\left[(\pi_x^1-\pi_y^1)/K\right]};$$

(ii) in family layer:

$$W\left(s_y \to s_x\right) = \frac{1}{1+\exp\left[\left(\pi_x^1 - \pi_y^1 + \frac{4b}{R_{\max}} \cdot \left(R_x^2 - R_y^2\right)\right)/K\right]}.$$

When configuring the Fermi functions, we adopt a primitive benefit-only formation for the social layer, as its existing disconnection–reconnection mechanism inherently mediates the effects of reputation effects on players' strategic choices. For the family layer, we design a dual-consideration Fermi function that integrates both payoff and reputation metrics, enabling the reputation system to directly incentivize strategic choices in familial relationships. In the family-layer Fermi function, in order to normalize the quantitative value we introduce the ratio $4b/R_{\max}$. In detail, $4b$ is the maximum possible payoff difference between two players in a round of the weak prisoner's dilemma. $R_{\max}$ is the maximum possible reputation difference between two players, and in this study, $R_{\max} = H = 40$.[31,32] For both layers, the parameter K represents the noise intensity, fixed at $K = 0.1$ in our simulations.

We employ asynchronous Monte Carlo simulations to model evolutionary dynamics on a dual-layer grid network ($L = 100$). The family-layer network comprises non-interconnected subgrids. Each MCS comprises T sequential operation time steps. Within each time step, the following operations are executed for every player: payoff calculation, reputation update and strategy update. At 10^5 MCS (ensuring equilibrium), we compute the average cooperation frequency F_c over the final 1000 steps. To reduce uncertainty, we conducted 20 independent experiments for each set of parameter values.

3. Simulation results and analysis

We systematically investigated the effects of three key parameters, namely, σ, α and b, on the cooperation frequency F_c. σ quantifies how players' individual reputations and the environmental reputation jointly modulate connection probabilities in the social layer. α represents the strength of the strategy persistence-consistency parameter d in reputation updates across both layers. b denotes the temptation-to-defect payoff in the prisoner's dilemma. The family-layer lattice is partitioned into non-overlapping 2×2 subgrids to model isolated family units. All subsequent family-layer analyses assume this partitioned subgrid structure unless noted.

Figure 2 shows the cooperation frequency F_c versus temptation b, under fixed σ and varying α. Figure 2(a), 2(b) and 2(c), 2(d) display the evolution trajectories for the social and family layers, respectively. At fixed σ and b, increasing the strategy persistence-consistency impact factor α enhances F_c in both layers. A higher α implies greater rewards and penalties for players' strategy persistence, resulting in a larger reputation gap between those who consistently choose to cooperate and those who consistently choose to defect. Consider $b = 1.4$: in the social layer, varying α values mean different reputation gaps even for players adopting identical strategies. A larger α exacerbates the difference in corresponding F_c as shown in Fig. 2(a). By contrast, in the family layer, the difference in F_c is relatively smaller (Fig. 2(c)). This is in line with real-life situations. Familial loyalty buffers against reputation-driven defection: members sustain cooperation with low-reputation kin through family responsibility, maintaining a relatively stable cooperation frequency.

Compared with the family layer, increasing σ from 1.2 to 1.4 accelerates the transition from full cooperation to full defection in the social layer as the temptation to defect (b) rises. This implies that higher σ values destabilize cooperation in the social layer. For example, in Figs. 2(a) and 2(c) with $\sigma = 1.2$, the curves corresponding to $\alpha = 1$ illustrate the following: for $b < 1.55$, the social layer sustains full cooperation ($F_c = 1$), whereas the family layer exhibits early defection ($F_c < 1$). As $b > 1.7$, social-layer cooperation frequency drops rapidly to 0.4 and gradually becomes a state of full defection, while the family layer can maintain $F_c > 0.4$ throughout. This demonstrates that under rising b, the social layer initially preserves full cooperation but collapses rapidly upon emergence of defection. In contrast, the family layer fails to sustain full cooperation initially but retains a state where cooperators and defectors coexist in the later stage. These divergent outcomes stem from distinct interaction mechanisms: dynamic social ties versus stable familial bonds.

To systematically compare evolutionary dynamics across the two layers, we employ heatmaps to visualize the effects of parameters α and b on cooperation. Given $\sigma = 1.2$, Fig. 3 depicts variations of F_c in the social layer (Figs. 3(a) and 3(b)) and the family layer (Figs. 3(c) and 3(d)) under different values of α and b. The social layer exhibits a larger full cooperation region (yellow area) than the family layer. Conversely, the family layer features a larger region of coexistence of cooperators and defectors. That is, it is relatively rare for everyone in a family to defect or cooperate, and more often there are both cooperators and defectors. In contrast, in the social layer, the situation where cooperators and defectors coexist is rarer, and the areas of full cooperation and full defection of the entire group are larger. At high b ($b > 1.8$), elevating α fails to prevent full defection in the social layer despite stronger rewards/punishments for strategy consistency. In the family layer, when b increases, increasing α accelerates the transition from full cooperation to mixed states but sustains partial cooperation even at high b. Figures 3(a) and 3(c) exhibit a consistent trend: color gradients transition from blue (low F_c) to yellow (high F_c) diagonally from top-left to bottom-right. This indicates that increasing parameter α and decreasing parameter b has a promoting effect on the cooperation of both the social and family layers.

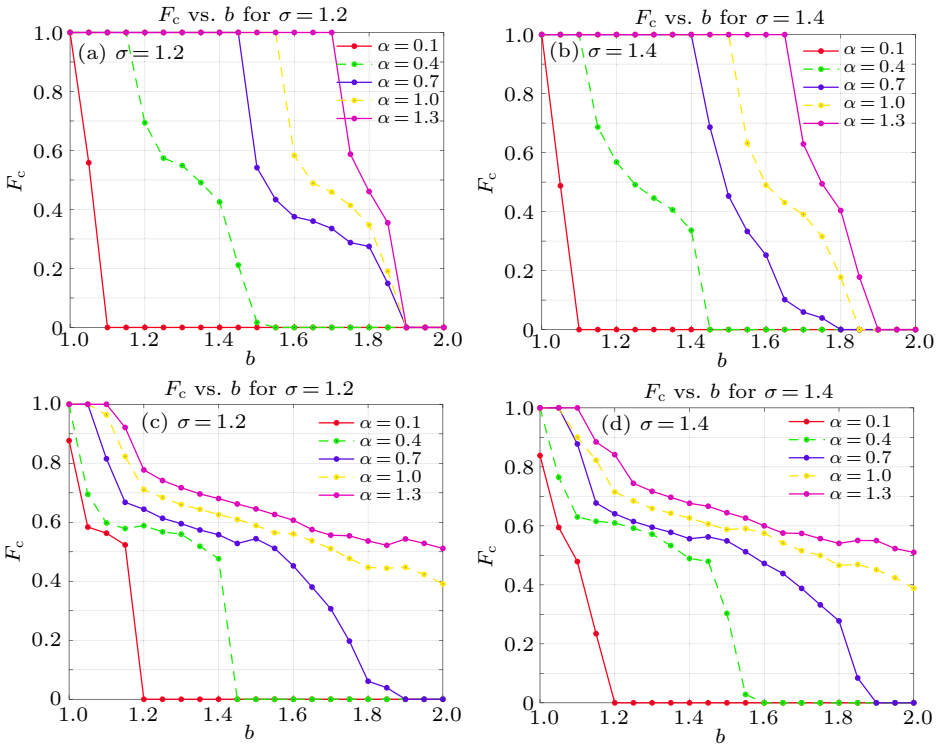


Fig. 2. Cooperation frequency F_c versus temptation-to-defect b in (a), (b) social and (c), (d) family layers, under varying disconnection–reconnection probabilities (σ) and strategy persistence-consistencies (α).

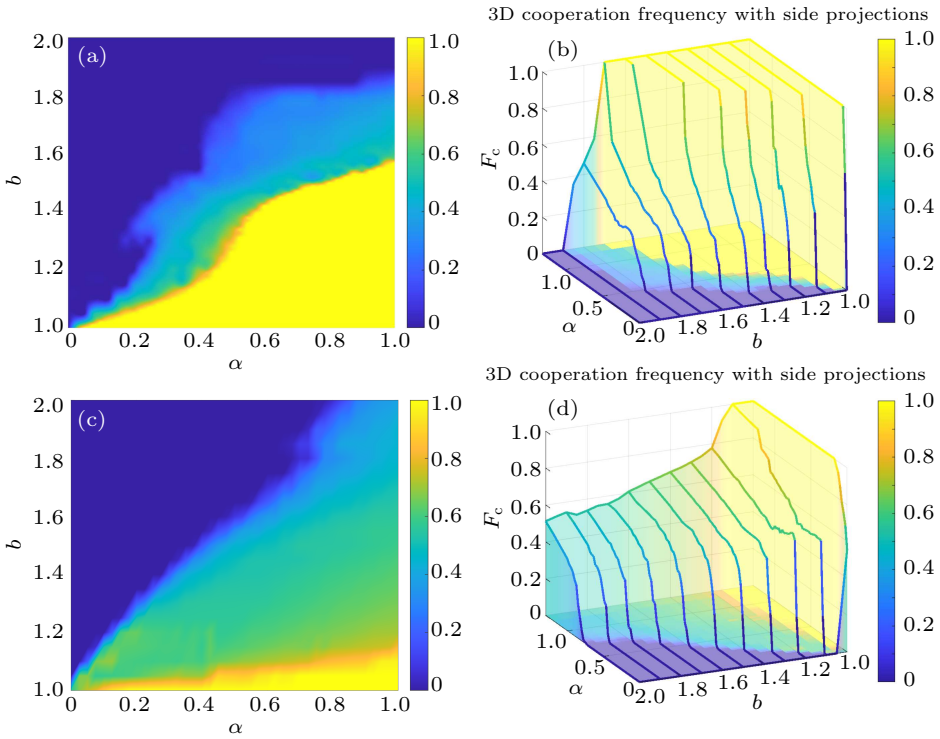


Fig. 3. Cooperation frequency F_c versus temptation-to-defect b and strategy persistence-consistency α in (a), (b) social and (c), (d) family layers.

We now focus on the snapshot diagrams of the evolutionary process, which capture the population state at multiple time points, enabling micro-level observation. Figure 4 illustrates the evolution of players' strategies and reputations under the parameter settings $b = 1.3$, $\sigma = 1.4$ and $\alpha = 0.4$. The first and second rows depict strategy selections and reputation values in the social layer, whereas the third and fourth rows correspond to those in the family layer. Initially, as the reputation mechanism has not yet reached full effect, most players exhibit defection tendencies. Notably, in the family layer, there is a large cluster of defectors at time $t = 10$. By contrast, the social layer employs a disconnection mechanism that promptly severs ties with low-reputation players, thereby effectively resisting defector invasion. In subsequent stages, as

the reputation mechanism gains efficacy, cooperators progressively form clusters, driving the system toward a stable state. Regarding reputation dynamics, both layers exhibit polarization: most individuals attain either the highest or lowest reputation values, with only a minority maintaining intermediate levels. In the final stable state, the social layer develops larger cooperator and defector clusters. However, in the family layer, due to its division into four small networks, both the clusters of cooperators and defector are relatively smaller and intermingled. However, in the family layer (partitioned into four subnetworks), both cooperator and defector clusters are comparatively smaller and interspersed.

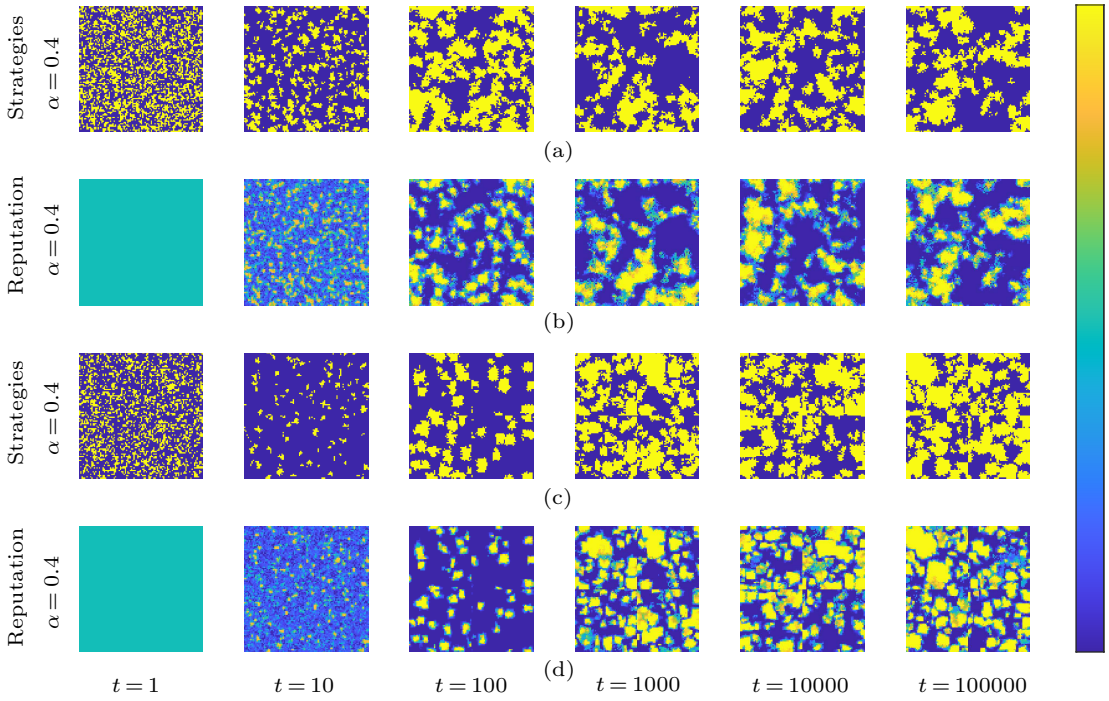


Fig. 4. Spatial snapshots of strategy choices and reputation values at different time steps t with $\alpha = 0.4$, $b = 1.3$ and $\sigma = 1.3$. Panels (a) and (b) display strategy selections and reputation values in the social layer, respectively, while panels (c) and (d) present the analogous data for the family layer. The time steps progress from the first column to the last column as 1, 10, 100, 1000, 10000 and 100000. In panels (a) and (c), yellow denotes cooperators while purple represents defectors. In panels (b) and (d), the color bar on the right indicates the variation in reputation values, with higher values corresponding to higher positions in the color bar.

Figure 5 presents the evolutionary snapshot diagram of players' strategies and reputations when parameters are set at $b = 1.3$, $\sigma = 1.4$ and $\alpha = 0.6$. Compared with Fig. 4, increasing α to 0.6 elevates the rate of cooperation in both layers. Cooperator clusters form more rapidly in both layers, ultimately converging to a state of coexistence of defectors and cooperators. It is evident that when α is set at 0.6, the population is in a more favorable state, with both layers ultimately converging to a higher level of cooperation. We can also observe a corresponding relationship between reputation and strategy. When the system reaches a stable state, cooperator clusters generally attain the maximum reputation value while defector clusters collectively stay at the minimum reputation value. Players at cluster edges, influenced by neighboring cooperators and defectors, experience frequent strategy changes. This causes the strategy persistence-consistency parameter d to reach 1, resulting in intermediate reputation values.

To investigate the strategy-switching behavior of players in the social layer, Fig. 6 illustrates the trend of strategy changes for four types of players during the evolution of the social layer. The parameter configuration in Fig. 5 is set to $b = 1.3$. Rows one to three are configured with $\alpha = 0.4$, $\alpha = 0.6$ and $\alpha = 0.8$, while columns correspond to $\sigma \to 0$, $\sigma = 1$, 1.2, 1.4, 1.6, 1.8 and $\sigma \to \infty$. A consistent phenomenon emerges across all sub-figures: during the initial $t = 10$ evolutionary steps, when the transition rate from cooperation to defection ($C \to D$) is lower than that from defection to cooperation ($D \to C$), the proportion of persistent defectors increases, whereas persistent cooperators decrease. As t increases and the reputation mechanism gains efficacy, persistent defectors decline in proportion, while persistent cooperators rise. When the $C \to D$ and $D \to C$ transition rates equilibrate and the proportions of persistent defectors and cooperators stabilize, indicating that the evolution has entered an oscillatory stable state. Furthermore, across all sub-figures, players transitioning between strategies consistently constitute a minority. As shown in Figs. 4 and 5, from $t > 10$ onward, defectors and cooperators aggregate into clusters rather than isolated points. This is because we use the Fermi rule to update players' strategies, so players in the middle of a cluster will always learn from their neighbors, that is, they will choose the strategy consistent with the cluster. Only at cluster boundaries — where players are

exposed to both strategies — do frequent strategy shifts occur. The interior regions of clusters occupy significantly larger areas compared with boundaries, explaining the persistently low proportion of strategy-transitioning players. This observation aligns with the analysis of Figs. 4 and 5. When a stable state is finally reached, the two types of players who persist in consistent strategies account for the majority of the population. This also indicates from another perspective that, at a stable state, reputations will not remain at intermediate values but will be polarized.

To further investigate the temporal evolution of the social layer, we analyze the relationship between parameters α, σ and b and the cooperation frequency F_c at each MCS. Figure 7 illustrates the temporal trend of the F_c of the social layer under four different α values, with σ and b varied across subfigures. From MCS $t = 1$ to $t = 100000$, F_c exhibits a slight decline within the first $t = 10$ steps, where the reputation mechanism remains ineffective. Beyond $t = 10$, in the first six columns, except for subfigures with $b = 1.6$, $\sigma = 1.6$ and $\sigma = 1.8$, F_c curves associated with higher α values exhibit

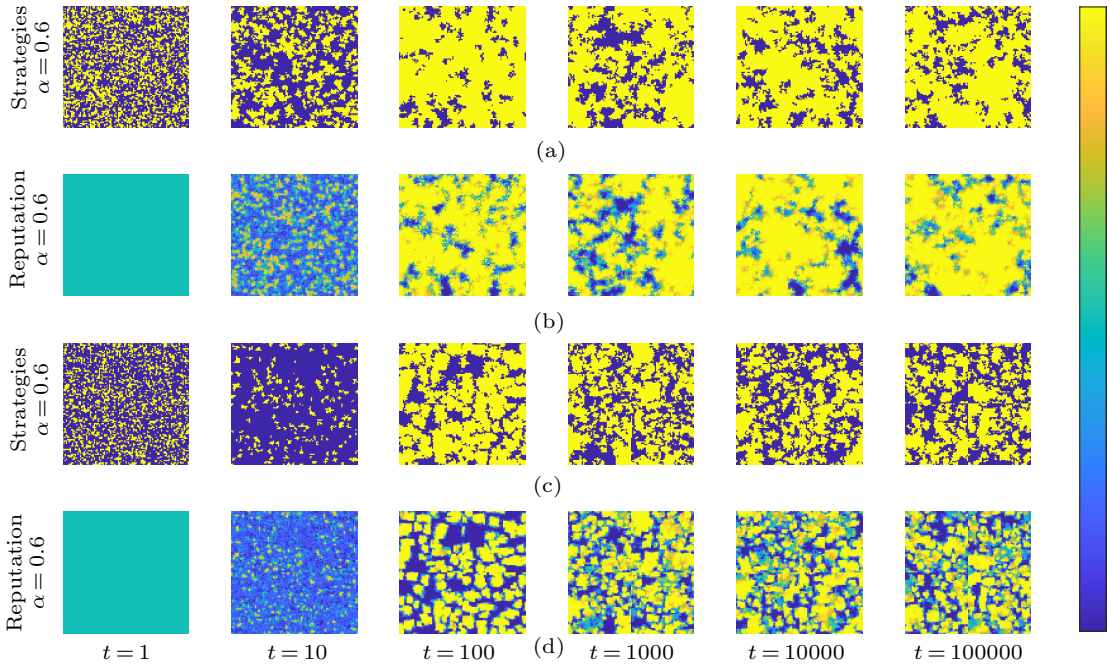


Fig. 5. Spatial snapshots of strategy choices and reputation values at different time steps t with $\alpha = 0.6$, $b = 1.3$ and $\sigma = 1.3$. Panels (a) and (b) display strategy selections and reputation values in the social layer, respectively, while panels (c) and (d) present the analogous data for the family layer.

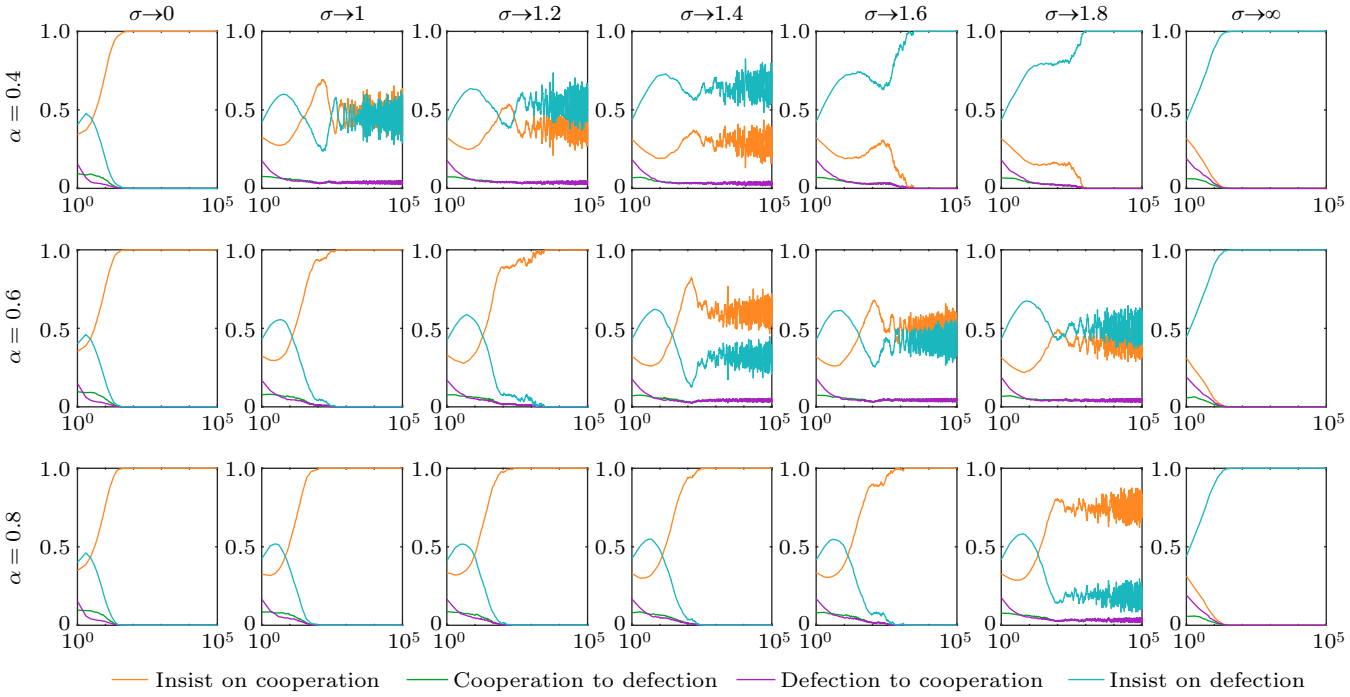


Fig. 6. Fractions of four transition states of players in the social layer as a function of the evolutionary time steps in MCS for different α and σ when $b = 1.4$.

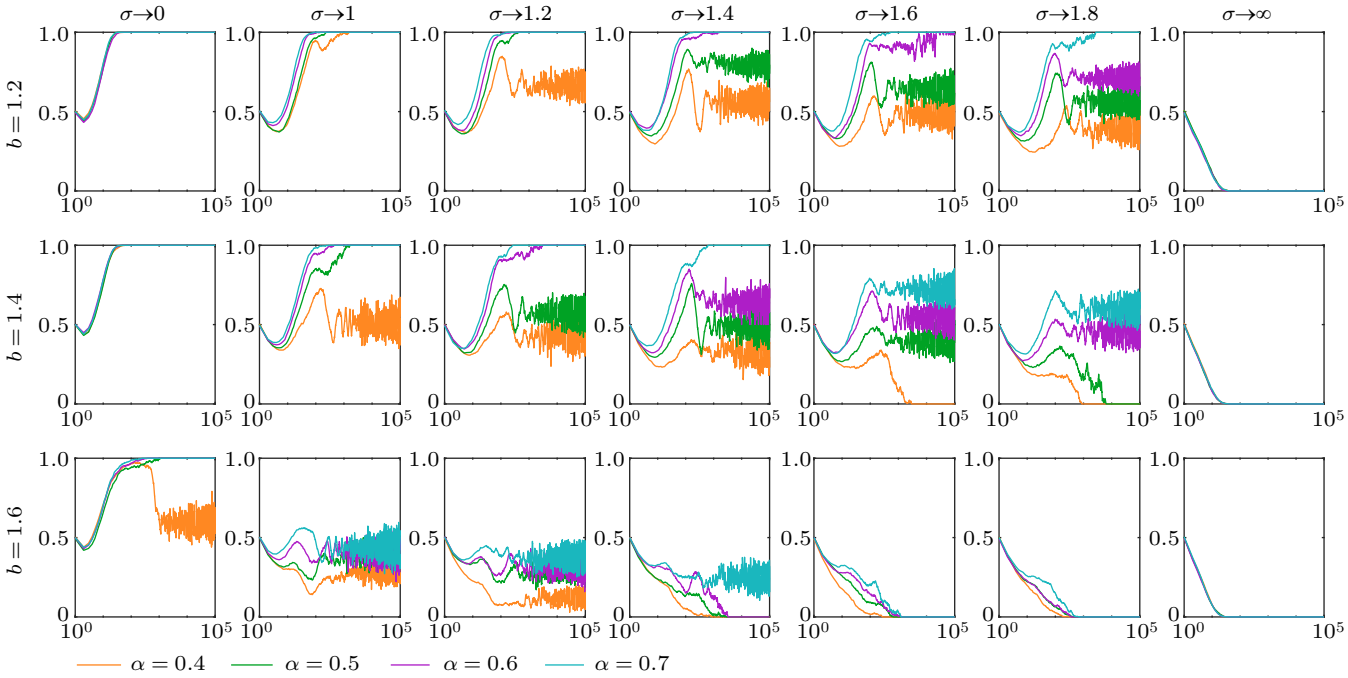


Fig. 7. Temporal evolution of F_c in the social layer under varying α, σ and b.

gradual increases. Notably, larger α accelerates the rise of F_c. By $t = 100$, F_c attains a relatively high level, with some curves (e.g., $b = 1.2$) achieving full cooperation ($F_c = 1$). Other F_c curves that fail to reach full cooperation show slight post-peak declines before stabilizing through oscillations. For curves with high σ and b but low α (e.g., $b = 1.6$ and $\sigma = 1.8$), or when $\sigma \to \infty$, defector proportions persist until $t = 10$ but eventually diminish to zero, resembling traditional prisoner's dilemma outcomes without reputation incentives. The F_c trends in Fig. 7 align with the proportions of persistent cooperators in Fig. 6. Thus, strategy-persistent players dominate the population and dictate the evolutionary trajectory.

Simultaneously, we observe F_c trends across seven σ value per row. Higher σ values correlate with oscillations and stabilizing at low F_c or converging to full defection. Conversely, lower σ values promote oscillations at high F_c or full cooperation. A higher σ implies a greater standard deviation in the normal distribution function in Eq. (4). This indicates that players are less sensitive to the difference between their average reputation and the environmental reputation. Consequently, the mechanism of disconnection and reconnection among players has a smaller impact, hindering the emergence of cooperation. Considering the two-edge case $\sigma \to 0$ and $\sigma \to \infty$, When $\sigma \to 0$, the probability density function of the normal distribution is an infinitely high vertical line at the mean. The distribution function is to the left of the mean and 1 at and to the right of the mean. In this case, if the average reputation of two players is less than the environmental reputation, and they will definitely disconnect. If the average reputation is greater than or equal to the environmental reputation they will definitely connect. This is an idealized situation. When $\sigma \to \infty$, whether players connect is purely random and reputation no longer affects connection probabilities. When $\sigma \to 0$ or $\sigma \to \infty$, the model is overly powerful or ineffective, so we view it as unrealistic. In social interactions, people usually consider not only reputation but also a variety of other factors when forming relationships, making the process more stochastic. Therefore, we choose a slightly larger value for σ, such as $\sigma = 1.2$, 1.4, 1.6, 1.8 or 2, where the normal distribution can better fit the reality.

For the family layer, since the disconnection and reconnection mechanism is not considered, we analyzed the trend of F_c under four different α values when $\sigma = 1.3$ and $b = 1.4$. As shown in Fig. 8, the overall trend of change in the family layer is consistent with that of the social layer, that is, the larger the α, the higher the F_c value in the final convergence state. However, unlike the social layer, the family layer requires a higher α to significantly increase the F_c. When $\alpha = 0.4$, the steady-state F_c value reaches approximately 0.5. To further increase F_c, a larger α is needed. For example, when α increases from 0.4 to 1.2, the steady-state F_c only rises from 0.5 to approximately 0.7. Similarly, when α is increases from 0.4 to 2, F_c can reach around 0.9. This indicates that, in the family layer, the reputation incentive mechanism can promote cooperation to some extent, but compared with the social layer a larger α is required to achieve a significant increase in cooperation. This suggests that influencing decisions through the Fermi function is more challenging than the disconnection and reconnection mechanism. In real-life scenarios, individuals may disconnect from an unfavorable social environment, but in families, cutting ties is generally not feasible. Therefore, harmonious fam-

ilies are rarer than cohesive work groups.

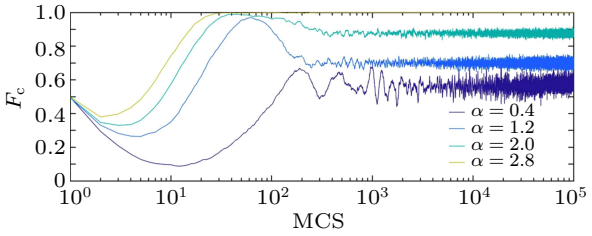


Fig. 8. Cooperation frequency F_c at each step of the Monte Carlo simulation in the family layer with varying α, where $b = 1.4$ and $\sigma = 1.3$. The curves (from bottom to top) correspond to $\alpha = 0.4$, $\alpha = 1.2$, $\alpha = 2$ and $\alpha = 2.8$.

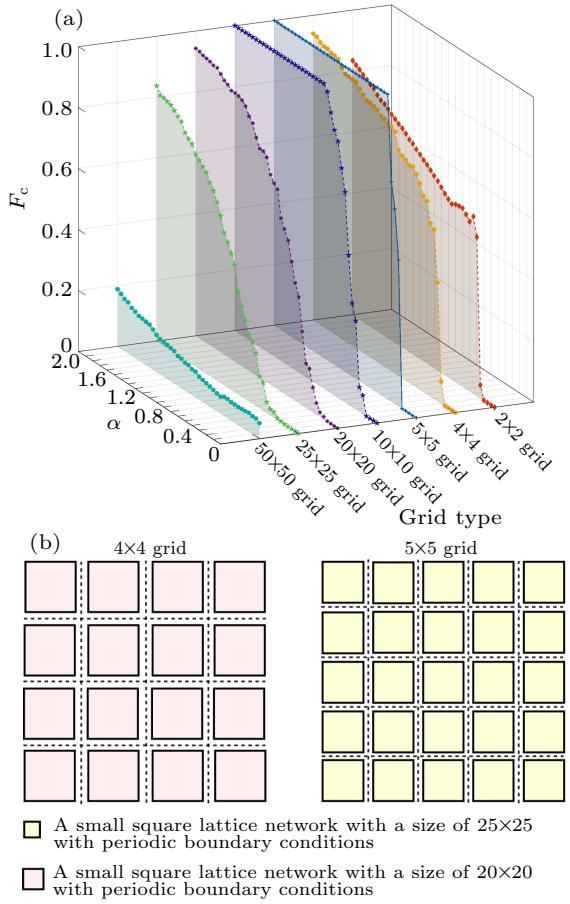


Fig. 9. Cooperation frequency F_c in the family layer varying with α under different specifications of small network structures.

To explore the effect of family size on cooperation frequency, the original 100×100 family layer network is divided into smaller grids to represent different family sizes. As shown in Fig. 9(a), we analyze how cooperation frequency varies with α across different grid types. Figure 9(b) illustrates divisions of 4×4 grids and 5×5 grids, with other grid divisions being similar. At $\sigma = 1.2$ and $b = 1.3$, all curves show an upward trend as α increases, indicating that the model in this study works across all family divisions, but with varying degrees of promotion on cooperation. Overall, the cooperation rate first rises and then falls as the family size decreases. The cooperation frequency peaks when the grid is divided into 5×5 grids of $20 \times 20 = 400$ players. This is because smaller networks facilitate the formation and spread of cooperator groups. However, over-subdivision can cause some small networks to quickly evolve to full cooperation or full defection, leading to evolutionary stagnation. When division is very fine, such as into 50×50 grid subnetworks, the cooperation frequency does not drop to even when α is very small. This is because all players' strategies are initially randomly assigned, and there are always subnetworks with four cooperators in the 2500 subnetworks. In subsequent evolution, these four people learn from each other using the Fermi rule and will never change to defectors.

4. Conclusion

We construct a dual-layer network model to simulate social and family relationship networks. We introduce a strategy persistence-consistency factor and a reputation update rule, allowing players to dynamically adjust their strategies based on reputation. In both network layers, players engage in games based on the payoff matrix of the weak prisoner's dilemma. In the social layer, players dynamically adjust their connections with neighbors based on reputation. Meanwhile, in the family layer, we introduce a dual-consideration Fermi function, enabling the reputation system to directly incentivize strategic choices within familial relationships. Within these mechanisms, the parameter σ represents the influence of the players' average reputation and environmental reputation on the probability of establishing connections, whereas α denotes the influence of the strategy persistence-consistency factor on reputation updates. The parameter b reflects the temptation to defect. Through simulations and analysis, we find that σ, α and b significantly influence the cooperation frequency. Specifically, the cooperation frequency is negatively correlated with σ and b but positively correlated with α. Our results demonstrate a significant enhancement in cooperation within the dual-layer network. Furthermore, to investigate the influence of family size on cooperation rates, we examine the evolutionary outcomes under different family network division patterns. The findings reveal that, within a certain range, smaller family sizes lead to higher rates of cooperation. This study provides new analytical perspectives for understanding cooperation dynamics in complex networks.

Our research connects the dual-layer network through a reputation incentive mechanism based on strategy persistence-consistency, while incorporating a disconnection–reconnection mechanism into the network structure. In future research, we could explore multi-layer networks with dynamic interlayer relationships. Additionally, the square lattice network analyzed in this study serves as a foundation for extending this framework to other complex networks, such as

small-world or scale-free networks, which represent promising directions for our future research.

Acknowledgement

This work was supported by the National Natural Science Foundation of China (Grant No. 72001207).

References

[1] Axelrod R and Hamilton W 1981 *Science* **211** 1390
[2] Szabó G and Tőke C 1998 *Phys. Rev. E* **58** 69
[3] Nowak M and Sigmund K 1993 *Nature* **364** 56
[4] Perc M and Szolnoki A 2008 *Phys. Rev. E* **77** 011904
[5] Press W H and Dyson F J 2012 *Proc. Natl. Acad. Sci. USA* **109** 10409
[6] Li J, Zhang J and Liu Q 2024 *Chin. Phys. B* **33** 030202
[7] Santos F C, Santos M D and Pacheco J M 2008 *Nature* **454** 213
[8] Wang Z, Szolnoki A and Perc M 2013 *Scientific Reports* **3** 1183
[9] Kang, Jin, Li, Wang, Sun, Yong and Chen 2023 *Chin. Phys. B* **33** 030203
[10] Wang X and Wang T 2023 *Chin. Phys. B* **32** 100202
[11] Hauert C and Doebeli M 2004 *Nature* **428** 643
[12] Wang W X, Ren J, Chen G and Wang B H 2006 *Phys. Rev. E* **74** 056113
[13] Doebeli M, Hauert C and Killingback T 2004 *Science* **306** 859
[14] Liu Y, Li Z, Chen X and Wang L 2010 *Physica A* **389** 2390
[15] Sun C and Luo C 2020 *Chaos, Solitons Fractals* **131** 109504
[16] Mo F and Han W 2024 *Appl. Math. Comput.* **476** 128786
[17] Sun X, Li M, Kang H, Shen Y and Chen Q 2023 *Appl. Math. Comput.* **445** 127853
[18] Jalal Eddine Bahbouhi, Saif Islam Bouderba, Abdelali Elkouay and Moussa N 2024 *Appl. Math. Comput.* **469** 128553
[19] Yang Z H and Yang Y L 2024 *Chin. Phys. B* **33** 090205
[20] Quan J, Chu Y Q, Liu W, Wang X J and Yang X K 2018 *Chin. Phys. B* **27** 060203
[21] Huang C, Li Y and Jiang L L 2023 *Phys. Rev. E* **108** 024123
[22] Yang K, Huang C, Dai Q and Yang J 2018 *Chaos, Solitons Fractals* **115** 23
[23] Shu F, Liu Y, Liu X and Zhou X 2019 *Appl. Math. Comput.* **346** 480
[24] Chen W, Wang J, Yu F, Xu W and Dai W 2024 *Appl. Math. Comput.* **473** 128639
[25] Bai X, Ye Y, Chen T and Xie N 2024 *Appl. Math. Comput.* **474** 128709
[26] Hu X, Li C and Huan M 2024 *Chaos, Solitons Fractals* **186** 115173
[27] Hu Q, Zhou M, Jiang Y and Liu X 2024 *Appl. Math. Comput.* **482** 128977
[28] Bi Y and Yang H 2023 *Appl. Math. Comput.* **444** 127818
[29] Shen Y, Yin W, Kang H, Zhang H and Wang M 2022 *Phys. Lett. A* **428** 127935
[30] Bi Y and Yang H 2023 *Physica A* **624** 128939
[31] He J, Wang J, Yu F and Zheng L 2020 *Phys. Lett. A* **384** 126703
[32] Zhang H, An T, Wang J, Wang L, An J, Zhao J and Jin X 2024 *Phys. Lett. A* **508** 129495
[33] Pei H, Yan G and Wang H 2021 *Chin. Phys. B* **30** 050203
[34] Wang Z, Wang L, Szolnoki A and Perc M 2015 *Eur. Phys. J. B* **88** 124
[35] Gómez-Gardeñes J, Romance M, Criado R, Vilone D and Sánchez A 2011 *Chaos* **21** 016113
[36] Perc M, Petek O and Kamal S M 2014 *Appl. Math. Comput.* **249** 19
[37] Wang H, Li Q, D'Agostino G, Havlin S, Stanley H E and Van Mieghem P 2013 *Phys. Rev. E* **88** 022801
[38] Aguirre J, Sevilla-Escoboza R, Gutiérrez R, Papo D and Buldú J M 2014 *Phys. Rev. Lett.* **112** 248701
[39] Guan J Y, Wu Z X, Huang Z G and Wang Y H 2010 *Chin. Phys. B* **19** 020203
[40] Luo C, Zhang X, Liu H and Shao R 2016 *Physica A* **450** 560
[41] Wang Z, Li C, Jin X, Ding H, Cui G and Yu L 2021 *Appl. Math. Comput.* **399** 126051
[42] Wang Z, Szolnoki A and Perc M 2013 *Scientific Reports* **3** 1183
[43] Su L, Yang Z, Zhou B, Zhang N and Li Y 2023 *Appl. Math. Comput.* **454** 128029
[44] Ma J and Zhao H 2024 *Appl. Math. Comput.* **479** 128863
[45] Wang C, Wang L, Wang J, Sun S and Xia C 2017 *Appl. Math. Comput.* **293** 18
[46] Nag Chowdhury S, Kundu S, Duh M, Perc M and Ghosh D 2020 *Entropy* **22** 485
[47] Ge X, He X, Yang J, Zhao Y, Liu Y and Li L 2024 *Scientific Reports* **14** 16932
[48] Yang P, Fan R, Wang Y and Zhang Y 2024 *Chin. Phys. B* **33** 070206
[49] Gómez S, Díaz-Guilera A, Gómez-Gardeñes J, Pérez-Vicente C J, Moreno Y and Arenas A 2013 *Phys. Rev. Lett.* **110** 028701
[50] Zimmermann M G, Eguíluz V M and San Miguel M 2004 *Phys. Rev. E* **69** 065102
[51] Gräser O, Xu C and Hui P M 2009 *Europhys. Lett.* **87** 38003
[52] Pan Q, Liu X, Bao H, Su Y and He M 2018 *Physica A* **492** 571
[53] Sakiyama T 2021 *Chaos, Solitons Fractals* **146** 110932
[54] Wang C, Lin Z and Rothman D S 2022 *Chaos, Solitons Fractals* **162** 112461
[55] Chen J, Liu X, Wang H and Yang J 2022 *Chaos, Solitons Fractals* **157** 111897
[56] Zhang Q, Liu J and Zhang X 2024 *Physica A* **650** 129999
[57] Wang J, He J and Yu F 2021 *Chaos, Solitons Fractals* **146** 110887